

## Measurement of the Average Equilibrium Charge of Fast Heavy Ions in a Solid by $H^+$ Emission at the Exit Surface

S. Della-Negra, Y. Le Beyec, B. Monart, and K. Standing<sup>(a)</sup>

*Institut de Physique Nucléaire, 91406 Orsay Cedex, France*

and

K. Wien

*Institut für Kernphysik, Technische Hochschule, Darmstadt, West Germany*

(Received 3 October 1986)

The  $H^+$  secondary-ion yield from the surface of solid targets of Au, C, and nitrocellulose has been used to measure mean charges of energetic ions of  $^{84}\text{Kr}$  and  $^{40}\text{Ar}$  (at 1.16 MeV/u) at the beam-exit surface. Values for Kr ions were found to be 1.6 to 3 electronic charges ( $e$ ) less than those found 70 ns later, after Auger decay. No such difference was observed for Ar ions of the same velocity.

PACS numbers: 34.50.Fa, 32.80.Hd, 34.70.+e

The behavior of the charge states of energetic ions passing through matter is a complex problem of considerable theoretical interest.<sup>1</sup> It also has important practical applications in heavy-ion physics, especially in accelerators. In solids, collisions which may change the charge state take place at time intervals of about  $10^{-16}$  s. So far the only source of information on the charge states inside the solid is x-ray emission from projectiles having vacancies in electronic orbitals.<sup>2,3</sup> These experiments, however, give only numbers of vacancies in inner shells. In the following, a new method is presented to determine the charge state of a projectile at the instant this projectile leaves a solid surface. For Kr ions this charge state is found to be smaller than the one reached after Auger decays in a vacuum; this is in qualitative agreement with the multiple-excitation model. This method uses the influence of charge states on yields of secondary  $H^+$  ions ejected from the surface when a fast ion intersects the surface.

The ejection of secondary ions from a solid by bombardment with heavy ions of 0.5–5 MeV/u is very sensitive to the charge state  $q$  of the primary projectile.<sup>4–10</sup> Yields of molecular ions from the target exhibit a fairly complex behavior; they depend on the atomic number of the bombarding ion as well as its charge. This has been explained in terms of the charge-exchange processes taking place at a depth of about 100–200 Å with the assumption that the yields depend on the integrated energy loss within that region.<sup>7–12</sup> On the other hand, yields  $Y$  of light atomic ions, particularly  $H^+$  or  $C^+$ , follow a very simple pattern; for a given projectile velocity they are independent of the bombarding ion—and therefore of the total energy lost in the foil—but depend only on its charge  $q$  when it crosses the surface.<sup>8–10</sup> In contrast to most molecular ions, the  $H^+$  emission is related to the high-energy density deposition in the vicinity of the projectile before energy dissipation. This energy is locally

dependent on the instantaneous charge state of the projectile.  $Y(H^+) \propto q^n$  with  $n \sim 3$  (see below). This suggests the use of the  $H^+$  yield as a sensitive probe of the projectile charge state at the surface.

Relatively large energy distributions of  $H^+$  ions emitted from a surface under MeV ion bombardment have been measured recently.<sup>13,14</sup> These results also lead to the conclusion that the  $H^+$  ion is “probing the internal environment of the ion track in the beginning of its evolution.”<sup>14</sup> In these later experiments  $H^+$  ions were observed from both the entrance and exit surface of the targets. The interaction distance between MeV primary ion and secondary ions is larger for molecular ions or atomic clusters than for  $H^+$  and  $C^+$ <sup>9</sup> ions but it is generally believed that in both cases direct atomic or molecular collisions with the projectile are not involved in the mechanism of desorption.

The experimental setup has been described completely elsewhere.<sup>10</sup> A beam from the Orsay heavy-ion linear accelerator passes through a thin C foil to produce a distribution of charge states. The charge state desired is selected by a magnet, and the resulting low-intensity ion beam ( $\sim 100$  ions/s) is collimated to 1 mm diameter before striking the target. Figure 1 shows a schematic diagram of the experimental geometry. After passing through the target, the energy of each ion is measured in a Si detector; an event is accepted only if the primary ion has the full energy expected.<sup>10</sup> A vacuum of about  $10^{-7}$  Torr is maintained in the system by a cryopump.

If an equilibrium charge-state distribution is required, an absorber can be inserted into the beam about 100 cm upstream from the target. In the experiments reported here, the absorber was always a foil of the same material and thickness as the target. The primary ions take about 70 ns to travel between the absorber and the target, so any excited states of short lifetime will have decayed by the time the ions strike the target.

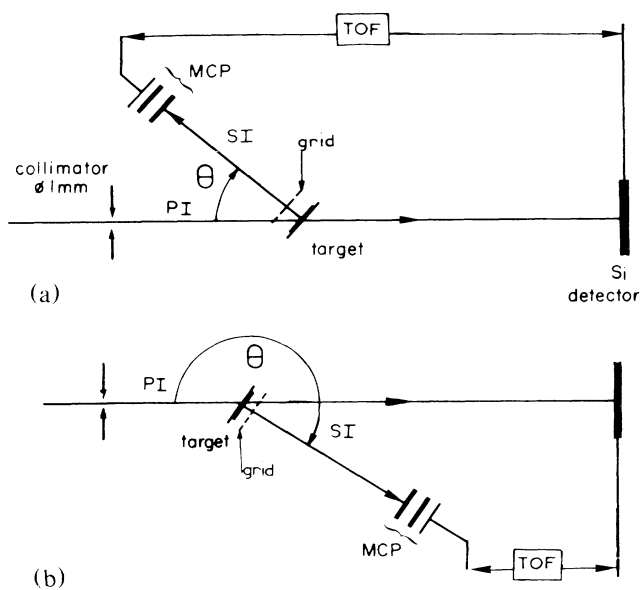


FIG. 1. Schematic diagram of the experimental arrangement showing the primary-ion beam (PI) and the ejected secondary ions (SI) observed in a microchannel plate detector (MCP). Secondary ions may be observed from the front as in (a), or from the back, as in (b).

Secondary ions emitted from the target are observed in a microchannel plate (MCP) detector. Their masses are measured by time of flight (the time interval between the Si detector "start" pulse and the MCP detector "stop" pulse) over a flight path of 15 cm. The target and the MCP detector are mounted on the same platform. It can be rotated from outside the chamber to change the angle of incidence of the primary beam. It can also be rotated through  $180^\circ$  to observe the secondary ions ejected either from the entrance or from the exit side of the target (i.e., before or after the primary beam passes through the target material), as shown in Figs. 1(a) and 1(b). Since the target and the detector move together, the secondary ions observed always originate from the same target surface, and the detector geometry is exactly the same for the two cases.

Thin foils of C, Au, and nitrocellulose ( $C_{12}H_{17}N_3O_{16}$ ) served as targets. The thicknesses of the nitrocellulose foils were measured by infrared absorption. The targets were bombarded by Ar or Kr ions of constant velocity (energy/nucleon = 1.16 MeV/u) and of charge state 7+ to 15+ for  $^{40}\text{Ar}$ , and 12+ to 25+ for  $^{84}\text{Kr}$ . High yields of  $\text{H}^+$  were observed in each case, so background was not a serious problem. Yields measured for a given target were found to be reproducible within 5% over a 24-h period. The projectile velocity dependence of the  $\text{H}^+$  yield has been measured around 1.16 MeV/u ( $v \sim 1.1$  cm/ns).<sup>15</sup> The foil thicknesses are such that the relative variations of ion velocities are around 1% for 1000 Å

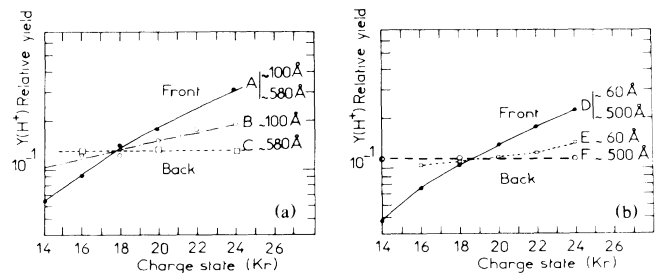


FIG. 2.  $\text{H}^+$  yields as a function of the charge state of the incident ion. (a) Nitrocellulose: A, 100 Å, front; B, 100 Å, back; C, 580 Å, back. (b) Carbon: D, 500 Å, front; E, 60 Å, back; F, 500 Å, back. The  $\text{H}^+$  yields for the different thicknesses 100 and 580 Å (nitrocellulose) and 500 and 60 Å (carbon) have been normalized from measurements of  $\text{H}^+$  emitted from the front at a given charge state. (The  $q$  dependence of the  $\text{H}^+$  yield is similar for different thicknesses when bombarded from the front.)

gold foil and smaller than 0.2% for 500-Å carbon foil. The corresponding yield and stopping power ( $dE/dx$ ) variations are negligible.

Figure 2(a) shows the  $\text{H}^+$  yields from a nitrocellulose target bombarded by Kr ions as a function of the Kr charge state. Curve A gives the results observed from the front, i.e., for the geometry of Fig. 1(a). As mentioned above, the yield varies as  $q^n$  with  $n \sim 3$ . The other two curves illustrate yields observed from the back, i.e., for the geometry of Fig. 1(b). For the 580-Å target the measured yields (curve C) are independent of the initial charge state, indicating that this target is thick enough to produce charge equilibrium. The constant  $\text{H}^+$  yield from curve C is thus a measure of the average equilibrium charge state  $q$  when the projectiles leave the target. The measured value of this quantity is slightly larger than the real value because of the width of the charge-state distribution and of the rapid increase of  $Y(\text{H}^+)$  with  $q$ . However, this effect is calculated to give an error of only a few percent. Since the projectiles have a velocity larger than  $10^{17}$  Å/s and since the yield curves suggest that the  $\text{H}^+$  yield measures the charge state within a distance much smaller than 100 Å from the surface, it is clear that the charge state is measured before any appreciable number of Auger decays (lifetime  $10^{-9}$ – $10^{-13}$  s) have occurred.

The value of  $q$  is determined by the intersection of curves A and C, provided there is no intrinsic front-back asymmetry like the one observed for a number of molecular ions.<sup>6,15</sup> In particular we have recently measured an enhancement of 40% for the yield of molecular ions emitted from the exit surface of a thin layer of phenylalanine (1000 Å evaporated on a 500-Å carbon foil). The incident Kr projectile was taken in its equilibrium charge state (18+, see later) but no difference between the exit and entrance surfaces has been observed

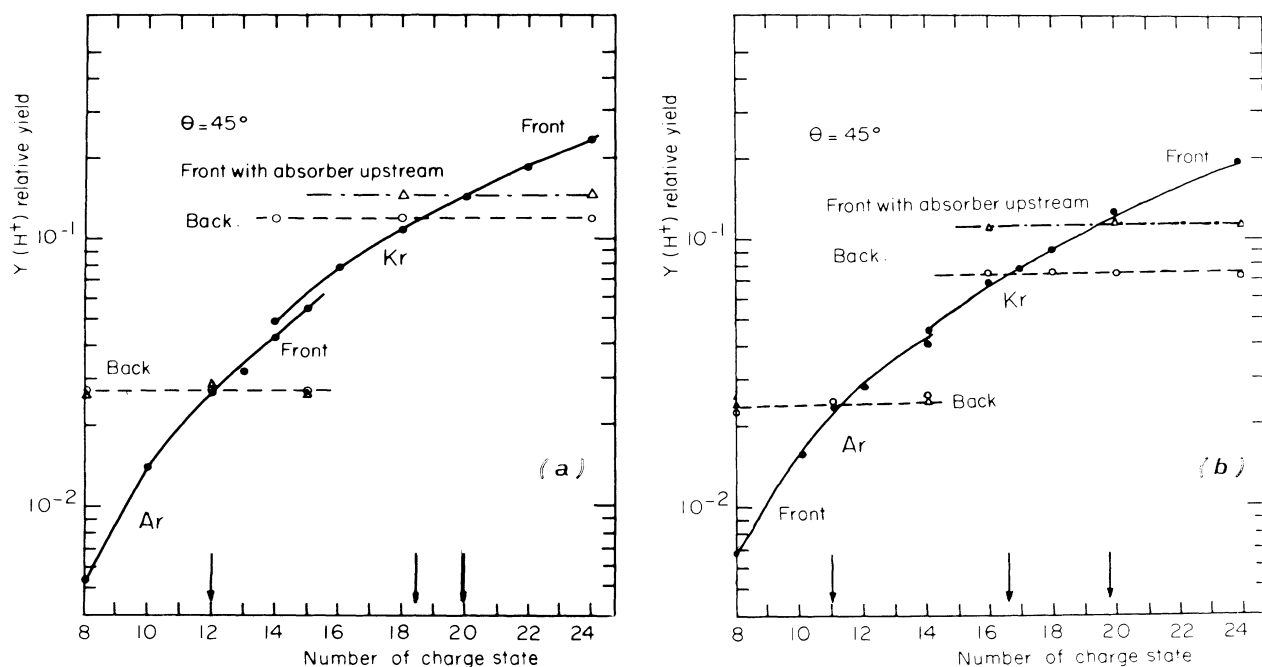


FIG. 3.  $H^+$  yields as a function of the charge state of the incident ion for (a) 500-Å carbon and (b) 1000-Å gold. In each case solid circles represent the front; triangles, the front with absorber upstream; and open circles, the back.

for the  $H^+$  yield. Furthermore, if such an asymmetry existed here for  $H^+$  ions, it would show up when the target thickness was reduced below the value needed to produce equilibrium; the point of intersection between curve *A* and curves measured from the back would change with target thickness. Curve *B* in Fig. 2 shows the yields measured for a 100-Å target. Clearly, charge-state equilibrium has not yet been reached for this target, but curves *A*, *B*, and *C* all intersect at the same point, corresponding to  $q \sim 18$ . We conclude that  $q \sim 18$  is the average equilibrium charge state of the primary beam at the exit surface of nitrocellulose. Similar arguments applied to the data for carbon in Fig. 2(b) lead to a value  $q \sim 18.4$  for the equilibrium charge state of the primary beam as it leaves a carbon foil.

The curves for the 500-Å carbon foil are plotted also in Fig. 3(a) along with corresponding data measured with an Ar beam. Also shown are the yields measured from the front when a 500-Å carbon absorber intercepted the beam at 100 cm upstream from the target. These determine the average equilibrium charge state  $q$  at a time 70 ns after the primary beam leaves the equilibrating foil. Our values agree with those measured by Baron under similar conditions.<sup>16</sup> For Ar bombardment the value of  $q$  ( $q = 12$ ) measured while leaving the foil agrees with the value measured 70 ns after leaving the similar absorber. For  $^{84}\text{Kr}$  bombardment there is a considerable difference, with  $\Delta q \sim 1.6e$ . Figure 3(b) shows similar measurements for a Au foil. The equilibrium

charge state for Kr ions leaving the Au surface is 16.6, but it is 19.7 when equilibrium is achieved in a gold foil upstream;  $\Delta q$  is thus  $\sim 3e$  [see Fig. 3(b)]. For Ar primary ions the values of  $q$  ( $q = 11.3$ ) in the two cases are again the same. The results are presented in Table I.

The observation that heavy-ion charge states were larger after the ion had passed through a solid than they were after passing through a gas was first explained by Bohr and Lindhart.<sup>17</sup> In their model the charge state inside the solid is equal to the mean charge state after leaving the solid, so no difference in  $H^+$  emission between front and back measurements would be expected for relatively thick target. More recently Betz and Grodzins have proposed a multiple-excitation model<sup>18</sup> which predicts Auger electron emission *after* the projectile leaves the solid. In this model the projectile charge

TABLE I. Equilibrium charge state for the primary ions Kr and Ar after Auger decay and at the exit surface.

Primary ion	Target	$q_{\text{eq}}$ after Auger decay	$q$ exit surface
Kr	Carbon foil	20	18
	Au foil	19.7	16.6
	Nitrocellulose foil		18
Ar	Carbon foil	12	12
	Au foil	11.3	11.3

state reaches its final value only after one or more Auger decays, so the charge state on leaving the solid is lower than the charge state measured later. Our measurements show clear evidence for this process in the case of Kr. This result is in qualitative agreement with the interpretation of gas-solid differences in stopping powers observed by Geissel *et al.* for uranium incident ions.<sup>19</sup> For low- $Z$  ions like Ar, the difference between the mean charge state in gases and solids is expected to be small at 1 MeV/u. This could explain that no difference in the mean charge state was observed for Ar, suggesting that multiple excitation is important only for projectiles of higher  $Z$ . The projectile which intersects the exit surface is in a highly electronic excited state compared to the entrance surface. The charge-state dependence on the  $H^+$  emission can thus be slightly different at the entrance and exit surfaces. It was difficult under the present experimental conditions to investigate this second-order effect on the desorption yield. However, as pointed out by Shima *et al.*<sup>20</sup> it is likely that the degree of the post-foil increase depends on the excited electron states of the projectile. Also the ion charge states which have been measured in this work agree relatively well with the most recent calculations from Maynard and Deutsch<sup>12</sup> who give the variation of the ion charge state with the distance of penetration inside a solid. These values are larger than the effective charge states which are the results of a parametrization (with use of an approximate formula for  $dE/dx$ ) and which are deduced from energy-loss determinations. We plan further measurements with our technique to give more quantitative information on the projectile charge state in the interior of a solid.

We thank F. Rocard for the infrared thickness measurements and R. Bimbot for helpful discussions. We also thank M. Denoit for his help in designing the vacuum time-of-flight chamber and the staff of the workshop for its construction. We are grateful for the efficient assistance of the Linac operating staff.

<sup>(a)</sup>Permanent address: Physics Department, University of Manitoba, Winnipeg, Canada.

<sup>1</sup>H. D. Betz, in *Atomic Physics: Accelerators*, edited by P. Richard, Methods of Experimental Physics Vol. 17 (Academic, New York, 1980), p. 73, and in *Applied Atomic Collision Physics*, edited by H. S. W. Massey *et al.*, Condensed Matter Vol. 4 (Academic, New York, 1983), p. 1.

<sup>2</sup>W. A. Schoenfeldt, Gesellschaft für Schwerionenforschung Report No. 81-7 (unpublished).

<sup>3</sup>K. Sevier, J. Phys. B **14**, 4065 (1981).

<sup>4</sup>P. Håkansson, E. Jayasinghe, A. Johansson, I. Kamensky, and B. Sundqvist, Phys. Rev. Lett. **47**, 1227 (1981).

<sup>5</sup>W. Guthier, O. Becker, S. Della-Negra, W. Knippelberg, Y. Le Beyec, U. Weikert, K. Wien, P. Wieser, and R. Wurster, Int. J. Mass Spectrom. Ion Phys. **53**, 185 (1983).

<sup>6</sup>C. K. Meins, J. E. Griffith, Y. Qiu, M. H. Mendenhall, L. E. Seiberling, and T. A. Tombrello, Radiat. Eff. **71**, 13 (1983).

<sup>7</sup>E. Nieschler, B. Nees, N. Bischof, H. Frölich, W. Tiereth, and H. Voit, Radiat. Eff. **83**, 121 (1984).

<sup>8</sup>O. Becker, W. Guthier, K. Wien, S. Della-Negra, and Y. Le Beyec, in *Ion Formation from Organic Solids (IFOS III)*, edited by A. Benninghoven, Springer Proceedings in Physics Vol. 9 (Springer, New York, 1986), p. 11.

<sup>9</sup>K. Wien, O. Becker, and W. Guthier, Radiat. Eff. **99**, 267 (1986).

<sup>10</sup>S. Della-Negra, O. Becker, R. Cotter, Y. Le Beyec, B. Monart, K. Standing, and K. Wien, Orsay Report No. IPNO-DRE-86-09, J. Phys. (Paris) (to be published).

<sup>11</sup>N. E. B. Cowern, Radiat. Eff. Lett. **76**, 1 (1983).

<sup>12</sup>C. Deutsch and G. Maynard, in Proceeding of the First Workshop on Physics of Small Systems, edited by E. Hilf and K. Wien, Lecture Notes in Physics (Springer, New York, to be published).

<sup>13</sup>N. Furstenu, W. Knippelberg, F. R. Krueger, G. Weis, and K. Wien, Z. Naturforsch. **32a**, 711 (1977).

<sup>14</sup>R. Macfarlane, J. C. Hill, and D. L. Jacobs, J. Trace Microprobe Tech. (to be published).

<sup>15</sup>O. Becker, S. Della-Negra, Y. Le Beyec, and K. Wien, Nucl. Instrum. Methods Phys. Res. Sect. B **16**, 321 (1986).

<sup>16</sup>E. Baron, thesis, Université Paris-Sud, 1975 (unpublished); E. Baron and B. Delaunay, Phys. Rev. A **12**, 40 (1975).

<sup>17</sup>N. Bohr and J. Lindhard, K. Dan. Vidensk. Selsk. Mat. Fys. Medd. **28**, No. 7 (1954).

<sup>18</sup>H. D. Betz and L. Grodzins, Phys. Rev. Lett. **25**, 211 (1970); H. D. Betz, Nucl. Instrum. Methods **132**, 19 (1976).

<sup>19</sup>H. Geissel, Y. Laichter, W. F. N. Schneider, and P. Armbruster, Phys. Lett. **88A**, 26 (1983).

<sup>20</sup>K. Shima, M. Kakuta, S. Fujioka, and T. Ishihara, Nucl. Instrum. Methods Phys. Res. Sect. B **14**, 275 (1986).